Transition Metal Chemistry (2019) 44:641–647
https://doi.org/10.1007/s11243-019-00328-0

Cobalt(II) and cobalt(III) coordination polymers constructed from flexible *bis*-imidazole and polycarboxyl co-ligands: syntheses, crystal structures and properties

Jiu-Fu Lu[1] · Xiao-Hu Yu[1] · Ke Zhou[1] · Soumendra Kumar Roy[1] · Si-Yu Yue[1] · Li Li[1] · Cai-Bin Zhao[1] · Ling-Xia Jin[1]

Received: 22 December 2018 / Accepted: 23 April 2019 / Published online: 30 April 2019

Abstract
Two metal coordination polymers, namely $\{[Co(1,3\text{-BIP})(OBA)]\cdot 0.5H_2O\}_n$ (SNUT-1) and $[Co_2(\mu\text{-}\eta^1{:}\eta^1\text{-}O_2)(1,3\text{-BIP})_2(PMA)]_n$ (SNUT-2), where 1,3-BIP = 1,3-bis(imidazol)propane, H_2OBA = 4,4′-oxybis(benzoate) and H_4PMA = benzene-1,2,4,5-tetracarboxylic acid, were prepared by hydrothermal methods. Single-crystal X-ray analysis revealed that the structure of SNUT-1 consists of a $3D \rightarrow 3D$ twofold interpenetrating network that can be described as a 4-connected uninodal net with $(6^5{\cdot}8)$ topology. The structure of SNUT-2 consists of a 3*D* framework which can be described as a (4,5)-connected binodal net with $(4^2{\cdot}6^3{\cdot}8^4{\cdot}10)$ $(3^3{\cdot}4^2{\cdot}5)$ topology. The gas adsorption properties of SNUT-1 and photocatalytic activity of SNUT-2 for the degradation of Rhodamine B have been explored.

Introduction

Metal coordination polymers (MCPs) are a source of much current interest because of their wide potential applications in photochemistry, gas adsorption, molecular magnetism, heterogeneous catalysis, and their intriguing crystal structures [1–5]. In recent years, the combined use of two distinct organic ligands has been found to be an effective method for the synthesis of MCPs, because of their rich coordination modes, including monodentate, bridging and chelating [6, 7]. To date, many MCPs have been prepared from carboxylate-type O-donors and amines or other N-donors. In particular, di- and polycarboxylic acids have been widely used as bridging ligands to construct coordination frameworks with versatile structures [8], and ligands such as 4,4′-oxybis(benzoate) (H_2OBA) are good candidates for construction of coordination polymers [9–12]. Also, benzene-1,2,4,5-tetracarboxylic acid (H_4PMA) exhibits variation in the possible binding modes of its four acid groups and a strong tendency to form large, tightly bound metal cluster aggregates, and it has therefore been applied as an organic component to construct porous coordination frameworks. Meanwhile, the bis(imidazole)propane (BIP) is a good choice of N-donor ligand, since the flexible nature of the spacer alkyl allows the ligand to bend and rotate when it coordinates to metal centers [13, 14], resulting in a range of structural diversity. In recent years, some examples have been reported for cobalt(III) complexes that are bridged by peroxide ion (O_2^{2-}) [15–18]. In the bridged peroxo-dinuclear compounds, four O_2^{2-} metal binding coordination modes were found: trans- and cis-$\mu\text{-}\eta^1{:}\eta^1$ (end-on), $\mu\text{-}\eta^2{:}\eta^2$ (side-on) and $\mu\text{-}\eta^2{:}\eta^2$ (end-on/side-on) bridging, as illustrated in Scheme 1.

In this paper, we report the synthesis of two new MCPs, $\{[Co(1,3\text{-BIP})(OBA)]\cdot 0.5H_2O\}_n$ (SNUT-1) and $[Co_2(\mu\text{-}\eta^1{:}\eta^1\text{-}O_2)(1,3\text{-BIP})_2(PMA)]_n$ (SNUT-2), constructed by using the same bis-imidazole ligand with different polycarboxylates as the mixed ligands. The simulated H_2 adsorption properties of SNUT-1 and photocatalytic properties of SNUT-2 have been investigated.

Electronic supplementary material The online version of this article (https://doi.org/10.1007/s11243-019-00328-0) contains supplementary material, which is available to authorized users.

✉ Jiu-Fu Lu
jiufulu@163.com

✉ Cai-Bin Zhao
zhaocb@snut.edu.cn

✉ Ling-Xia Jin
jinlx@snut.edu.cn

[1] Shaanxi Province Key Laboratory of Catalytic Foundation and Application, College of Chemical & Environment Science, Shaanxi University of Technology, Hanzhong 723001, People's Republic of China

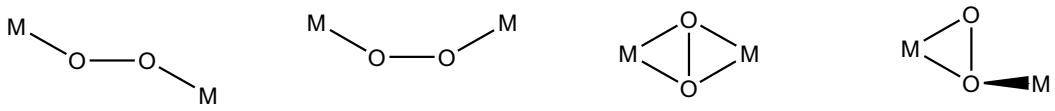

End-on bridging (trans) End-on bridging (cis) Side-on bridging End-on/Side-on bridging

Scheme 1 Binding modes in dinuclear bridged peroxo complexes

Experimental

Materials and physical measurements

All reagents used in the syntheses were of analytical grade and used without further purification. Powder X-ray diffraction (PXRD) data were collected on a Bruker D8 advance X-ray diffractometer with Cu Kα radiation ($\lambda = 1.54184$ Å), and the simulated powder patterns were calculated with the Mercury software package. Elemental analyses for carbon, hydrogen, and nitrogen atoms were obtained on a Vario EL III elemental analyzer. Infrared spectra (4000–400 cm^{-1}) were recorded using KBr pellets on an Avatar 360 E.S.P. IR spectrometer. Thermogravimetric analysis (TGA) was performed on a TA-SDT Q600 thermal analyzer under N_2 atmosphere with a heating rate of 10 °C min^{-1} in the range of 30–1000 °C. Topology analysis for both complexes was carried out with the Topos4.0 program package. The UV–Vis spectra were obtained on a Shimadzu UV 2550 spectrometer.

Synthesis of SNUT-1

A solution of 4,4′-oxybis(benzoate) (0.10 mmol, 25.8 mg), 1,3-bis(imidazol)propane (0.10 mmol, 17.6 mg) and $Co(NO_3)_2{\cdot}6H_2O$ (0.10 mmol, 29.1 mg) in distilled water (15 mL) was placed in a Teflon-lined stainless steel vessel, heated to 130 °C for 3 days and then cooled to room temperature over 24 h. The resulting solid was washed with methanol and dried under vacuum. Purple block crystals of SNUT-1 were obtained with a yield of 68% based on cobalt. Elemental analysis (%): calcd for $C_{23}H_{21}N_4O_{5.5}Co$ ($M = 500.37$): C, 55.16; H, 4.20; N, 11.19. found: C, 55.36; H, 4.12; N, 11.41. IR (cm^{-1}): 3440 (s), 3125 (w), 2917 (w), 1617 (s), 1558 (m), 1500 (w), 1423 (m), 1350 (m), 1270 (w), 1153 (w), 1091 (w), 997 (w) and 721 (m).

Synthesis of SNUT-2

The preparation of SNUT-2 was similar to that of SNUT-1 except that 4,4′-oxybis(benzoate) was replaced by benzene-1,2,4,5-tetracarboxylic acid (0.05 mmol, 11.3 mg). Pink block crystals of SNUT-2 were obtained. Yield: 72% based on cobalt. Elemental analysis (%): calcd for $C_{28}H_{26}Co_2N_8O_{10}$ ($Mr = 752.43$): C 46.25, H 3.46, N 14.89; found: C 46.21, H 3.81, N 14.38. IR (cm^{-1}): 3456 (m), 3125 (w), 2940 (w), 1588 (s), 1519 (m), 1501 (w), 1425 (m), 1371 (m), 1094 (m), 938 (m), 859 (m) and 755 (m).

Determination of crystal structures

Crystals of SNUT-1 (dimensions $0.22 \times 0.16 \times 0.14$ mm^3) and SNUT-2 (dimensions $0.26 \times 0.21 \times 0.14$ mm^3) were selected under an optical microscope. Data collections were performed at 293 K on a Bruker Smart Apex-II CCD area detector using graphite-monochromated Mo$K\alpha$ radiation ($\lambda = 0.71073$ Å). Each crystal was mounted on a glass fiber. The structures were solved by direct methods with the SHELXS-97 program [19] and refined by SHELXL-97 [20] using full-matrix least-squares techniques on F^2. All non-hydrogen atoms except the guest molecules were refined by full-matrix least-squares techniques with anisotropic displacement parameters. The hydrogen atoms were geometrically fixed at calculated positions attached to their parent atoms, and treated as riding. Crystallographic data for both complexes are presented in Table 1. Selected bond lengths and angles are listed in Table 2. CCDC data files 1025981 and 1001812 contain the supplementary crystallographic data for this paper.

Results and discussion

Structure of SNUT-1

Single X-ray diffraction study revealed that the asymmetric unit of SNUT-1, $\{[Co(1,3\text{-BIP})(OBA)]{\cdot}0.5H_2O\}_n$, contains one Co(II) atom, one OBA ligand, one 1,3-BIP ligand and half an H_2O molecule. As shown in Fig. 1a, each Co(II) atom is six-coordinated in a distorted octahedral geometry provided by two cis-nitrogen atoms from two 1,3-BIP ligands and four oxygen atoms from two OBA ligands. The adjacent Co centers are bridged by V-shaped OBA ligands to form a 1*D* right-handed $\{[Co(OBA)]\}_n$ single helical chain (Fig. 1b), such that the distance between adjacent Co(II) atoms is 14.3347 Å. Meanwhile, the 1,3-BIP ligand acts

Table 1 Crystallographic data and structure refinement for 1 and 2

Compounds	1	2
Formula	$C_{30}H_{25}CoN_4O_6$	$C_{28}H_{26}Co_2N_8O_{10}$
Fw	500.37	752.43
T/K	293 (2)	0.26 × 0.21 × 0.14
Crystal system	Orthorhombic	Monoclinic
Space group	*Fdd2*	*P2*(1)*/n*
a/Å	19.2130 (9)	12.0534 (6)
b/Å	52.3437 (19)	10.0111 (4)
c/Å	8.7523 (4)	12.2291 (7)
α/°	90	90.00
β/°	90	94.349 (6)
γ/°	90	90.00
V/Å^3	1.510	1471.41 (13)
Z	16	2
Dc/g cm^{-3}	1.510	1.662
F (000)	4128	752
GOF on F^2	1.065	1.029
Reflection/unique	5185/3660	5861/2571
R_1, $wR_2[I > 2\ (I)]$	0.0349, 0.0669	0.0530, 0.1258
R_1, wR_2 (all data)	0.0388, 0.0699	0.0613, 0.1314

$R_1 = \sum(||F_o| - |F_c||)/\sum|F_o|$, $wR_2 = [\sum(||F_o|^2 - |F_c||^2)^2/\sum w(F_o^2)]^{1/2}$

as an exo-bidentate linker, coordinating to Co(II) atoms to form a helical chain (Fig. 1b). These 1*D* left-handed helical chains are further connected by the helical chains to generate a 3*D* framework with one-dimensional channels, with internal dimensions of ca. 14.3347 × 10.5563 Å^2 along the c axis (Fig. 1c). Mutual interpenetration of two independent equivalent frameworks leads to the formation of a twofold parallel interpenetrating architecture (Fig. 1d). From a topological perspective, the Co(II) atom can be considered as a 4-connected uninodal net with a Schläfli symbol of (6^5·8).

Structure of SNUT-2

X-ray analysis reveals that the asymmetric unit of SNUT-2, $[Co_2(\mu\text{-}\eta^1\text{:}\eta^1\text{-}O_2)(1,3\text{-BIP})_2(PMA)]_n$, contains two Co(III) atoms, one PMA ligand, two 1,3-BIP ligands and one μ_2-O_2^{2-} ligand. During synthesis, the Co(II) starting material has been oxidized by molecular oxygen which is reduced to the peroxide ion, O_2^{2-} that bridges the two Co(III) centers. As illustrated in Fig. 2a, atoms Co1 and Co2 are both six-coordinated by four oxygen atoms from two PMA ligands and one μ_2-O_2^{2-} ligand, plus two nitrogen atom from two trans-1,3-BIP ligands, giving distorted octahedral geometries. Each PMA ligand is coordinated to four Co(III) atoms through deprotonated carboxylate groups to form a 2*D* $[Co_2(PMA)]_n$ layer (Fig. 2b). Adjacent 2*D* $[Co_2(PMA)]_n$

Table 2 Selected bond lengths (Å) and angles (°) for 1 and 2

1			
Co(1)–N(1)	2.073 (3)	Co(1)–N(4)	2.074 (3)
Co(1)–O(1)	2.181 (3)	Co(1)–O(3)	2.269 (2)
Co(1)–O(2)	2.155 (3)	Co(1)–O(4)	2.106 (2)
N(2)–Co(1)–O(1)	97.84 (11)	N(4)–Co(1)–O(3)	87.60 (11)
N(4)–Co(1)–O(1)	154.00 (11)	N(2)–Co(1)–O(2)	102.89 (11)
N(2)–Co(1)–O(3)	153.99 (10)	N(4)–Co(1)–O(4)	102.52 (12)
N(2)–Co(1)–N(4)	97.96 (12)	N(4)–Co(1)–O(2)	95.99 (12)
N(2)–Co(1)–O(4)	94.16 (10)	O(1)–Co(1)–O(4)	96.78 (10)
O(2)–Co(1)–O(4)	152.80 (11)	O(3)–Co(1)–O(4)	59.85 (9)
O(1)–Co(1)–O(2)	60.32 (11)	O(1)–Co(1)–O(3)	87.18 (11)
2			
Co(1)–N(1)	2.046 (3)	Co(1)–O(5)	2.316 (5)
Co(1)–N(4)	2.025 (3)	Co(1)–O(3)	2.107 (2)
Co(1)–O(1)	2.031 (3)	Co(1)–O(4)	2.324 (3)
O(5)–O(6)	1.654 (10)	N(1)–Co(1)–O(5)	81.07 (17)
N(4)–Co(1)–O(1)	96.79 (13)	O(1)–Co(1)–O(3)	102.20 (14)
N(4)–Co(1)–N(1)	156.27 (15)	N(1)–Co(1)–O(3)	95.72 (12)
N(1)–Co(1)–O(1)	97.89 (13)	N(4)–Co(1)–O(5)	78.04 (18)
N(4)–Co(1)–O(3)	99.28 (13)	O(1)–Co(1)–O(5)	100.27 (18)
O(5)–Co(1)–O(3)	157.53 (15)	N(4)–Co(1)–O(4)	85.57 (11)
O(1)–Co(1)–O(4)	161.19 (15)	N(1)–Co(1)–O(4)	86.51 (11)
O(3)–Co(1)–O(4)	59.06 (9)	O(5)–Co(1)–O(4)	98.48 (15)

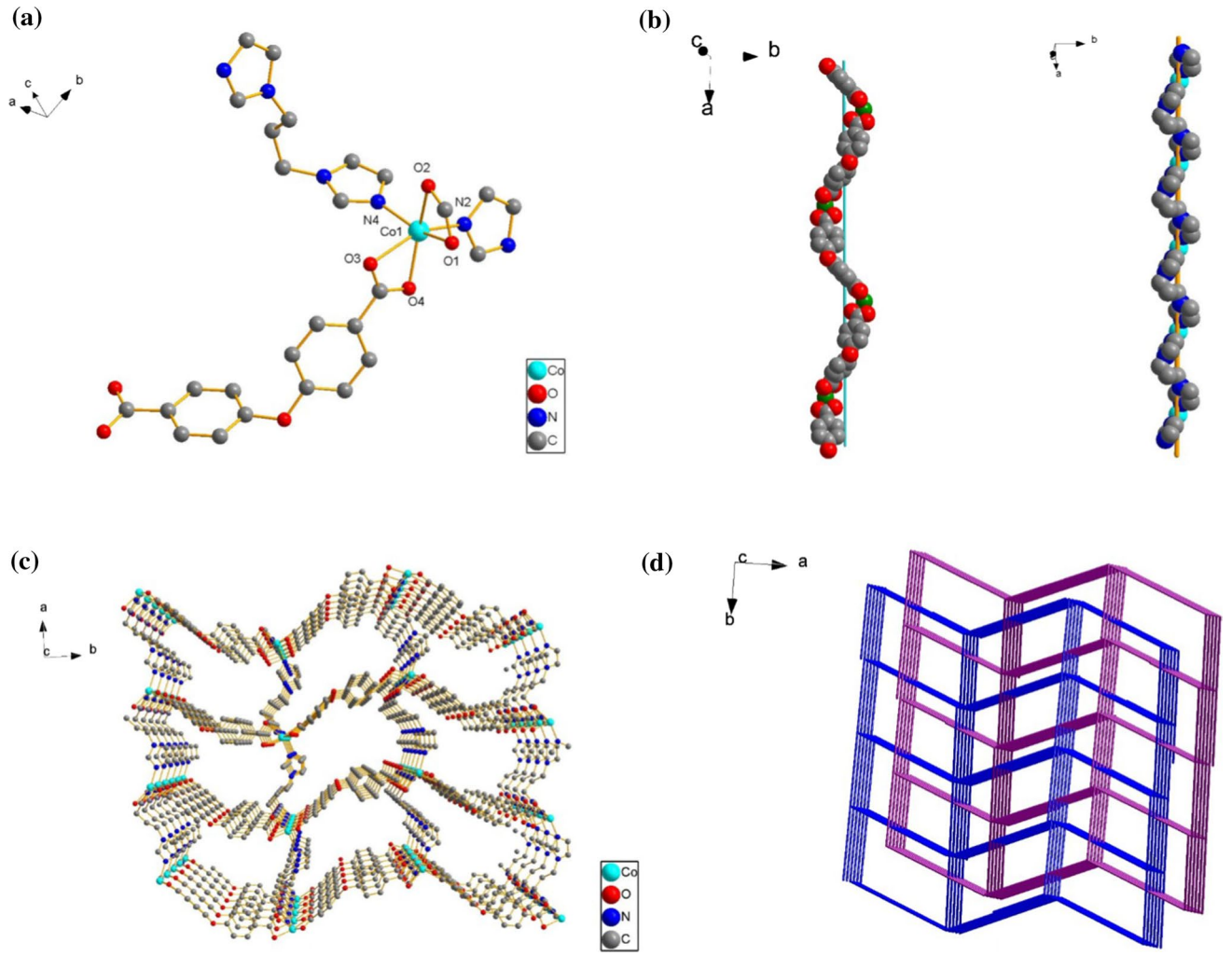

Fig. 1 **a** Coordination environment of the Co atom in SNUT-1 (the hydrogen and H_2O molecule are omitted for clarity); **b** view of two kinds of 1*D* helical chain; **c** view of 3*D* framework in 1; **d** perspective view of twofold $3D \rightarrow 3D$ parallel interpenetrating structure of 1. (Color figure online)

layers are further connected by the μ_2-O_2^{2-} ligands to generate a 3*D* framework with 1*D* channels with internal dimensions of ca. 9.6527×10.2153 Å^2 lying in the ab plane (Fig. 2c). The 3*D* framework is further elaborated by trans-1,3-BIP ligands to form a novel complicated architecture. From the topological perspective, the PMA ligands can be simplified as topologically equivalent 4-connected nodes, and each Co(III) atom as a 5-connected node (Fig. 2d). In this way, a binodal (4,5)-connected network is formed with a point symbol of $(4^2 \cdot 6^3 \cdot 8^4 \cdot 10)$ $(3^3 \cdot 4^2 \cdot 5)$.

Spectroscopic and physical properties

The FTIR spectra of SNUT-1 and SNUT-2 are shown in Fig. S1; strong broad bands centered at 3440 cm^{-1} for SNUT-1 can be attributed to the O–H stretching vibrations of water. The absence of strong peaks around 1720 cm^{-1} in the spectra of both complexes indicates that all carboxylic groups of OBA and PMA ligands are deprotonated. A strong peak at 1617 cm^{-1} for SNUT-1 indicates the presence of deprotonated –COO^- groups, while peaks at 1588 and 1425 cm^{-1} for SNUT-1 correspond to the asymmetric and symmetric vibrations of the carboxylate groups. The difference between these bands is less than 200 cm^{-1}, indicating that the carboxylate groups adopt chelate coordination modes [21]. The band appearing at 2940 cm^{-1} for SNUT-2 is assigned to the CH_2 groups. The bands between 1588 and 1371 cm^{-1} can be assigned to the asymmetric, ν_{as}(COO) and symmetric, ν_a(COO) vibrations of the coordinated carboxylate groups. The peroxo O–O stretching frequency, ν(O–O), was observed as a medium intense band at 755 cm^{-1} which is in the same range as that reported previously for structurally characterized dinuclear end-on bridged Co(III) complexes [22].

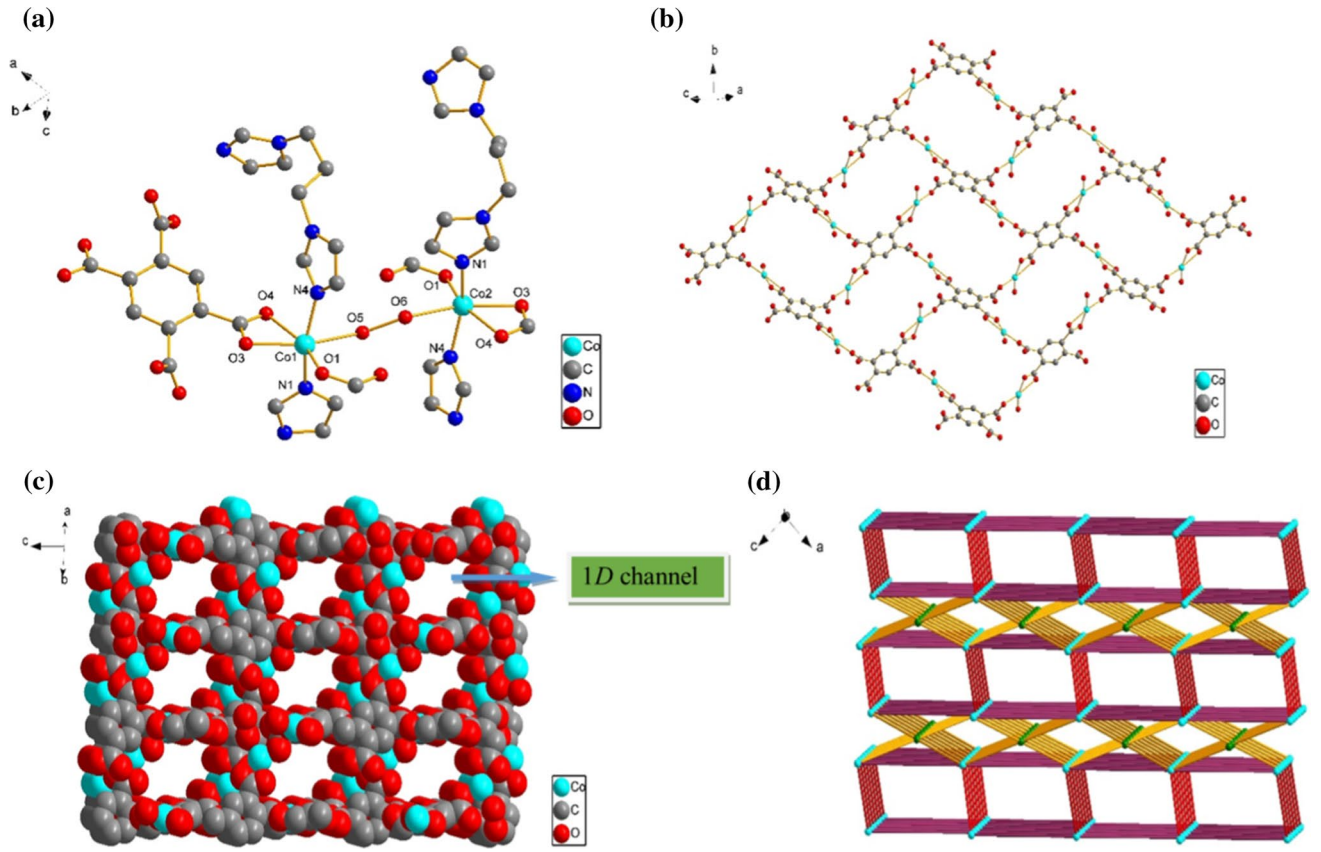

Fig. 2 **a** View of the coordination environment of the Co(III) atom of 2; **b** 2*D* layer constructed by Co(III) and PMA ligand; **c** 3*D* framework constructed by $[Co_2PMA]_n$ layer and μ_2-O_2^{2-}; **d** schematic view of the topology (PMA ligand represented as green ball, Co(III) atom represented as sky blue ball, BIP represented as purple rod, carboxyl of PMA ligands represented as yellow rod and μ_2-peroxo represented as red rod). (Color figure online)

Figure S2 shows the powder XRD patterns of as-synthesized compounds together with the simulated patterns on the basis of single-crystal structures. The good agreement between the observed and calculated patterns is an indicator of the phase purity of the as-synthesized bulk sample.

These MCPs were also analyzed by thermogravimetric analysis (TGA) from 30 to 1000 °C at a heating rate of 10 °C/min. Based on the TG curve depicted in Fig. S3, from room temperature to 67 °C, the TGA curve of SNUT-1 displays a slight weight loss of 1.94% (calcd: 1.58%), corresponding to half a water molecule. The framework is then stable up to 250 °C, after which it begins to collapse, accompanied by loss of the 1,3-BIP and OBA ligands. The residue is stable up to 1000 °C with a residual weight of 15.54% which may be attributed to CoO (calcd: 14.98%). SNUT-2 shows a slight weight loss of 3.6% in the temperature range of 30–410 °C, and it can be ascribed to the loss of one μ_2-O_2 ligand per unit cell (calcd: 4.2%). At higher temperatures, the framework begins to collapse, with loss of the 1,3-BIP and PMA ligands. The residue is stable to 1000 °C; its residual weight of 22.1% may be attributed to Co_2O_3 (Calcd: 22.0%).

Molecular simulation of SNUT-1

In order to assess the potential of SNUT-1 in gas storage applications, molecular simulations were performed. Using the Materials Studio Software Package, conventional grand canonical Monte Carlo (GCMC) simulation [23], which has been verified to be a reliable method for the simulation of gas adsorption, was used to explore the adsorption of H_2 by SNUT-1. The experimental crystallographic structure was used for the GCMC simulation. The universal force field (UFF) [24] was employed for the crystal atoms, since a number of studies have shown that the UFF gives reasonable agreement with experimental measurement [25]. The non-bond energies were calculated with the Ewald and Group method with a cutoff distance of 15.5 Å, and the Ewald accuracy was set to 1×10^{-4} kcal/mol. In addition, periodic boundary conditions were applied. The size of the simulation

box was set to 3 × 3 × 3 unit cells. The adsorption temperature was set at 77 K, and fugacity was increased from 10 to 100 kpa in order to obtain the adsorption isotherms of H_2. Simulations included a 1.0×10^6 cycle equilibration period followed by a 1.0×10^6 cycle production run. The results of the adsorption simulations are shown in Fig. 3. Our molecular simulations show that the H_2 adsorption of SNUT-1 conforms to the Langmuir mechanism under low pressure, and the saturated adsorption is as high as 67 mL g^{-1} (standard state) with an adsorption heat of − 13.2 kJ mol^{-1}. For comparison, we also computed adsorption isotherms at room temperature. As expected, the adsorbed amounts of H_2 reduce as the temperature increases. At room temperature, H_2 isotherms were away from saturation, since only a small amount of molecules were adsorbed, whereas at 77 K the H_2 isotherms approached saturation loading. In addition, the density field analysis shows that the H_2 is inclined to locate at the middle of the structure cavities, rather than being absorbed on the internal surface (Fig. 4). Overall, the molecular simulations indicate that the SNUT-1 synthesized in this work can be considered as a potential candidate for gas storage applications.

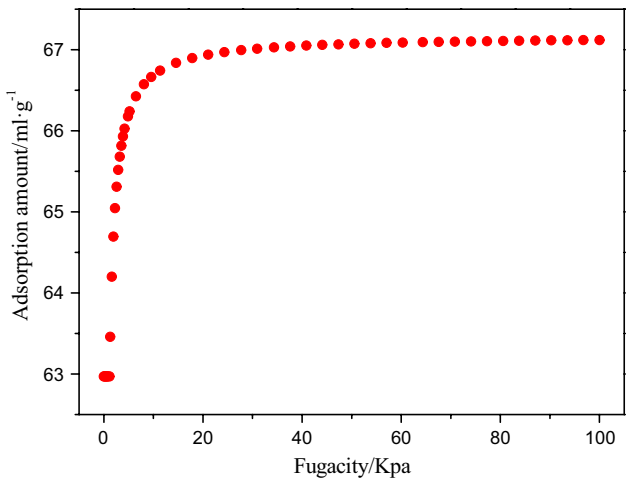

Fig. 3 Single-component H_2 uptake of SNUT-1 computed from GCMC simulations as a function of fugacity

Photocatalytic properties of SNUT-2

In general, the mechanism of photocatalytic degradation of rhodamine B (RhB) by MCPs is associated with semiconductor theory [26]. Previous studies have suggested that electron transfer from the photoexcited organic ligand to the metal (LMCT) within MCPs accounts for their photocatalytic activity [27]. Inspired by the previously reported studies on Co(II)/Cu(II) coordination polymers for photocatalytic degradation of organic dyes [28, 29], herein the photocatalytic activity of SNUT-2 for degradation of RhB under xenon arc lamp irradiation was explored. The characteristic adsorption peak of RhB at about 554 nm was selected to monitor the photocatalytic degradation process. As shown in Fig. S4, as the irradiation time was increased from 0 to 60 min, the intensities of the peaks at 554 nm decreased gradually, indicating that SNUT-2 has photocatalytic activity. As shown in Fig. 5, when the irradiation time reached 60 min, almost 79.1% of RhB was degraded, compared to

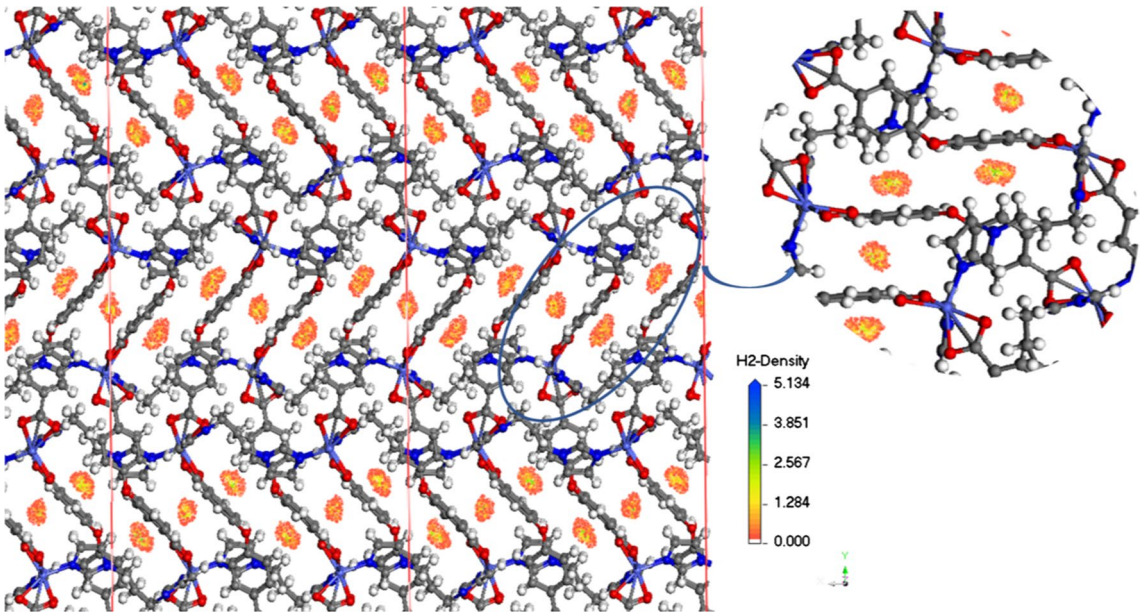

Fig. 4 A view of H_2 molecules in the hollows of SNUT-1. (Color figure online)

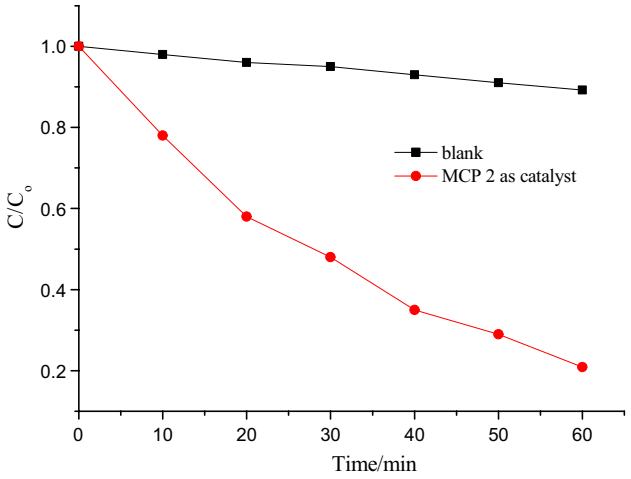

Fig. 5 Photocatalytic degradation of RhB solution under visible-light irradiation with the use of SNUT-2. The black curve is the control experiment without any catalyst. (Color figure online)

9% for a blank experiment. Hence, SNUT-2 can be used as a visible-light photocatalyst for the degradation of RhB.

Conclusions

In this work, two coordination polymers based on cobalt and 1,3-BIP mixed ligands have been prepared and characterized. SNUT-1 has a $3D \rightarrow 3D$ twofold interpenetrating network with $(6^5 \cdot 8)$ topology, while SNUT-2 has a $3D$ framework with $(4^2 \cdot 6^3 \cdot 8^4 \cdot 10)$ $(3^3 \cdot 4^2 \cdot 5)$ topology. The results of molecular simulations indicate that SNUT-1 may have potential for H_2 storage, while SNUT-2 has photocatalytic activity for degradation of RhB. Further experiments exploring the structural effects of the spacer length of bis(imidazole) ligands on the resulting coordination polymers, and the resulting variation in physicochemical properties, are under way in our laboratory.

Acknowledgements This work is supported by catalytic conversion team of syngas of Shaanxi University of Technology, National Youth Natural Science Foundation of China (Project No. 21603133), Key scientific research project of education department of Shaanxi province (18JS023, 17JS027), the project of Shaanxi provincial science and technology department (2018JM2043) and the Science Foundation of Shaanxi University of Technology (SLGQD2017-14, SLGKYQD2-08).

References

1. Eddaoudi M, Moler DB, Li HL, Yaghi OM (2001) Acc Chem Res 34:319–330
2. Halder GJ, Kepert CJ, Moubaraki B, Murray KS, Cashion JD (2002) Science 298:1762–1769
3. Dybtsev DN, Chun H, Yoon SH, Kim D, Kim K (2004) J Am Chem Soc 126:32–33
4. Kesanli B, Cui Y, Smith MR, Bittner EW, Bockrath BC, Lin WB (2005) Angew Chem Int Ed 44:72–75
5. Ghosh AK, Jana AD, Ghoshal D, Mostafa G, Chaudhuri NR (2006) Cryst Growth Des 6:701–707
6. Anokhina EV, Vougo-Zanda M, Wang XQ, Jacobson AJ (2005) J Am Chem Soc 127:15000–15001
7. Pan L, Parker B, Huang XY, Olson DH, Lee JY, Li J (2006) J Am Chem Soc 128:4180–4181
8. Xu B, Xie J, Hu HM, Yang XL, Dong FX, Yang ML, Xue GL (2014) Cryst Growth Des 14:1629–1641
9. Yin PX, Zhang J, Li ZJ, Qin YY, Cheng JK, Zhang L, Yao YG (2009) Cryst Growth Des 94:884–4896
10. Wang RH, Hong MC, Luo JH, Cao R, Weng JB (2003) Chem Commun 8:1018–1019
11. Zhang XM, Tong ML, Gong ML, Lee HK, Luo L, Li KF, Chen XM (2002) Eur J Chem 8:3187–3194
12. Montney MR, Supkowski RM, LaDuca RL (2008) CrystEngComm 10:111–116
13. Wen LL, Li YZ, Lu ZD, Lin JG, Duan CY, Meng QJ (2006) Cryst Growth Des 6:530–537
14. Fan J, Slebodnick C, Angel R, Hanson BE (2005) Inorg Chem 44:552–558
15. Febee RL, Lam TN, Albering B, Franz A, Mautner C, Salah S (2012) Inorg Chem Commun 15:269–271
16. Yamanari K, Mori M, Dogi S, Fuyuhiro A (1994) Inorg Chem 33:4807–4812
17. Tanase T, Onaka T, Nakagoshi M, Kinoshita I, Shibata K, Doe M, Fujii J, Yano S (1999) Inorg Chem 38:3150–3159
18. Mukherjee A, Cranswick MA, Chakrbarti M, Paine TK, Fujisawa K, Münck E, Que L (2010) Inorg Chem 49:3618–3625
19. Sheldrick GM (1997) A program for the Siemens area detector absorption correction. University of Gottingen, Gottingen
20. Sheldrick GM (1997) SHELXS 97 program for solution of crystal structures. University of Gottingen, Gottingen
21. Nakamoto K (1997) Infrared and Raman spectra of inorganic and coordination compound, 5th edn. Wiley, New York
22. Salah SM, Febee RL, Lam TN, Masahiro M, Jorg H, Albering FA (2011) Inorg Chim Acta 366:394–398
23. Frenkel D, Smit B (2002) Understanding molecular simulation: from algorithms to applications. Academic Press, 2nd edn, San Diego
24. Rappe A, Casewit C, Colwell K, Skiff W (1992) J Am Chem Soc 114:10024
25. Keskin S, Liu J, Rankin RB, Johnson JK, Sholl DS (2008) Ind Eng Chem Res 48:2355–2359
26. Silva CG, Corma A, García H (2010) J Mater Chem 20:3141
27. Zhang M, Wang L, Zeng T (2018) Dalton Trans 47:4251
28. Lu JF, Wang MZ, Liu ZH (2015) J Mol Struct 1098:41
29. Lu JF, Jin LX, Song J, Zhao CB, Yue SY, Li L, Yang HT, Cao XY, Ge HG (2018) Chin J Struct Chem 37:1814